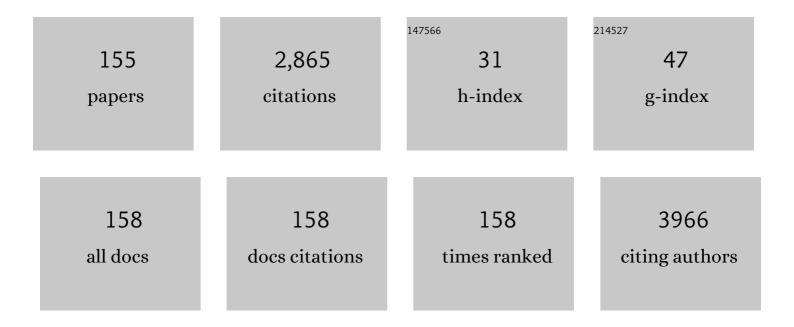
Hyung-Kook Kim

List of Publications by Year in descending order

Source: https://exaly.com/author-pdf/9562699/publications.pdf Version: 2024-02-01



HVUNG-KOOK KIM

#	Article	IF	CITATIONS
1	Nanogenerators facilitated piezoelectric and flexoelectric characterizations for bioinspired energy harvesting materials. Nano Energy, 2021, 81, 105607.	8.2	18
2	WO3–ZnO and CuO–ZnO nanocomposites as highly efficient photoanodes under visible light illumination. Nanotechnology, 2020, 31, 255702.	1.3	6
3	Controlled in situ capacitance sensing of single cell via simultaneous optical tweezing. Sensors and Actuators B: Chemical, 2020, 321, 128512.	4.0	3
4	A Comparative Study of the Effects of Different Methods for Preparing RGO/Metal-Oxide Nanocomposite Electrodes on Supercapacitor Performance. Journal of the Korean Physical Society, 2020, 76, 264-272.	0.3	4
5	Efficient and hysteresis-less perovskite and organic solar cells by employing donor-acceptor type Ï€-conjugated polymer. Organic Electronics, 2019, 72, 18-24.	1.4	25
6	Characterization of performance parameters of organic solar cells with a buffer ZnO layer. Advances in Natural Sciences: Nanoscience and Nanotechnology, 2019, 10, 015005.	0.7	5
7	Heat Generation by Ion Friction in Water under an AC Electric Field. Journal of the Korean Physical Society, 2019, 75, 832-840.	0.3	2
8	Water-Through Triboelectric Nanogenerator Based on Ti-Mesh for Harvesting Liquid Flow. Journal of the Korean Physical Society, 2018, 72, 499-503.	0.3	27
9	Exploring the use of impedance spectroscopy in relaxation and electrochemical studies. Applied Spectroscopy Reviews, 2018, 53, 157-176.	3.4	4
10	Scalable and inexpensive strategy to fabricate CuO/ZnO nanowire heterojunction for efficient photoinduced water splitting. Journal of Materials Science, 2018, 53, 2725-2734.	1.7	17
11	New 2D-Conjugated Polymer for Non-Halogenated and Halogenated Solvents Processed Organic Solar Cells. Macromolecular Research, 2018, 26, 1276-1279.	1.0	9
12	Versatile nanodot-patterned Gore-Tex fabric for multiple energy harvesting in wearable and aerodynamic nanogenerators. Nano Energy, 2018, 54, 209-217.	8.2	45
13	Aerodynamic and aeroelastic flutters driven triboelectric nanogenerators for harvesting broadband airflow energy. Nano Energy, 2017, 33, 476-484.	8.2	81
14	Spectroscopic study of binding of chlorogenic acid with the surface of ZnO nanoparticles. Russian Journal of Physical Chemistry A, 2017, 91, 1781-1790.	0.1	3
15	TiO ₂ Thin Films Sensitized with Upconversion Phosphor for Efficient Solar Water Splitting. Journal of Nanoscience and Nanotechnology, 2017, 17, 7647-7650.	0.9	7
16	Eu, Gd-Codoped Yttria Nanoprobes for Optical and T1-Weighted Magnetic Resonance Imaging. Nanomaterials, 2017, 7, 35.	1.9	28
17	Ratiometric pH Sensor Based on Fluorescent Core–Shell Nanoparticles. Journal of Nanoscience and Nanotechnology, 2017, 17, 8313-8316.	0.9	5
18	Inhibitory effect of traditional oriental medicine-derived monoamine oxidase B inhibitor on radioresistance of non-small cell lung cancer. Scientific Reports, 2016, 6, 21986.	1.6	37

#	Article	IF	CITATIONS
19	Effect of Er3+ and Yb3+ co-doping on the performance of a ZnO-based DSSC. Journal of the Korean Physical Society, 2016, 68, 1381-1389.	0.3	3
20	Effects of solvent polarity on the absorption and fluorescence spectra of chlorogenic acid and caffeic acid compounds: determination of the dipole moments. Luminescence, 2016, 31, 118-126.	1.5	30
21	Binding of caffeine with caffeic acid and chlorogenic acid using fluorescence quenching, UV/vis and FTIR spectroscopic techniques. Luminescence, 2016, 31, 565-572.	1.5	42
22	Cu-doped flower-like hematite nanostructures for efficient water splitting applications. Journal of Physics and Chemistry of Solids, 2016, 98, 283-289.	1.9	45
23	A flexible lead-free piezoelectric nanogenerator based on vertically aligned BaTiO3 nanotube arrays on a Ti-mesh substrate. RSC Advances, 2016, 6, 81426-81435.	1.7	26
24	Pt-coated TiO 2 nanorods for photoelectrochemical water splitting applications. Results in Physics, 2016, 6, 373-376.	2.0	34
25	Preparation of ZnO Nanorod/Graphene/ZnO Nanorod Epitaxial Double Heterostructure for Piezoelectrical Nanogenerator by Using Preheating Hydrothermal. Journal of Visualized Experiments, 2016, , e53491.	0.2	3
26	Probing the interaction of caffeic acid with ZnO nanoparticles. Luminescence, 2016, 31, 654-659.	1.5	13
27	Highly Durable Ti-Mesh Based Triboelectric Nanogenerator for Self-Powered Device Applications. Journal of Nanoscience and Nanotechnology, 2016, 16, 4864-4869.	0.9	9
28	Multicolor nanoprobes based on silica-coated gadolinium oxide nanoparticles with highly reduced toxicity. RSC Advances, 2016, 6, 19758-19762.	1.7	26
29	TiO2 nanofiber/nanoparticles composite photoelectrodes with improved light harvesting ability for dye-sensitized solar cells. Electrochimica Acta, 2016, 193, 166-171.	2.6	26
30	Effect of the dielectric layer on the electrical output of a ZnO nanosheet-based nanogenerator. Journal of the Korean Physical Society, 2015, 67, 1920-1924.	0.3	12
31	Fabrication of carbon coated gadolinia particles for dual-mode magnetic resonance and fluorescence imaging. Journal of Advanced Ceramics, 2015, 4, 118-122.	8.9	15
32	Freestanding ZnO nanorod/graphene/ZnO nanorod epitaxial double heterostructure for improved piezoelectric nanogenerators. Nano Energy, 2015, 12, 268-277.	8.2	72
33	Ti-doped hematite thin films for efficient water splitting. Applied Physics A: Materials Science and Processing, 2015, 118, 1539-1542.	1.1	28
34	Dye-sensitized solar cells composed of photoactive composite photoelectrodes with enhanced solar energy conversion efficiency. Journal of Materials Chemistry A, 2015, 3, 11130-11136.	5.2	27
35	Dual-mode spectral convertors as a simple approach for the enhancement of hematite's solar water splitting efficiency. Applied Physics A: Materials Science and Processing, 2015, 119, 1373-1377.	1.1	16
36	Bioinspired piezoelectric nanogenerators based on vertically aligned phage nanopillars. Energy and Environmental Science, 2015, 8, 3198-3203.	15.6	115

#	Article	IF	CITATIONS
37	Highly sensitive detection of epidermal growth factor receptor expression levels using a capacitance sensor. Sensors and Actuators B: Chemical, 2015, 209, 438-443.	4.0	15
38	Effects of Li ⁺ Codoping on the Optical Properties of SrAl _{2} O _{4} Long Afterglow Ceramic Phosphors. Advances in Optics, 2014, 2014, 1-4.	0.3	6
39	Effects of N- and N-In doping on ZnO films prepared by using ultrasonic spray pyrolysis. Journal of the Korean Physical Society, 2014, 65, 1890-1895.	0.3	2
40	Synthesis and physical properties of zinc-oxide textured films by using a filtered preheated hydrothermal. Journal of the Korean Physical Society, 2014, 65, 1423-1429.	0.3	2
41	Synthesis and Characterization of Flower-Like Bundles of ZnO Nanosheets by a Surfactant-Free Hydrothermal Process. Journal of Nanomaterials, 2014, 2014, 1-11.	1.5	34
42	Energy harvesting of dye-sensitized solar cells assisted with Ti-mesh and phosphor materials. IOP Conference Series: Materials Science and Engineering, 2014, 54, 012025.	0.3	4
43	Discrimination of Defective (Full Black, Full Sour and Immature) and Nondefective Coffee Beans by Their Physical Properties. Journal of Food Process Engineering, 2014, 37, 524-532.	1.5	10
44	Ultrafine PEG-capped gadolinia nanoparticles: cytotoxicity and potential biomedical applications for MRI and luminescent imaging. RSC Advances, 2014, 4, 34343-34349.	1.7	31
45	Luminescent core–shell Fe3O4@Gd2O3:Er3+, Li+ composite particles with enhanced optical properties. Journal of Sol-Gel Science and Technology, 2014, 71, 391-395.	1.1	22
46	Effects of Al–Mn coâ€doping on magnetic properties of semiconducting oxide thin films. Physica Status Solidi (B): Basic Research, 2014, 251, 2274-2278.	0.7	8
47	Improvement of Electrodeposition Rate of Cu Layer by Heat Treatment of Electroless Cu Seed Layer. Korean Journal of Materials Research, 2014, 24, 186-193.	0.1	0
48	Mesoporous silica with fibrous morphology: a multifunctional core–shell platform for biomedical applications. Nanotechnology, 2013, 24, 345603.	1.3	43
49	Enhanced Sunlight Harvesting of Dye-Sensitized Solar Cells Assisted with Long Persistent Phosphor Materials. Journal of Physical Chemistry C, 2013, 117, 17894-17900.	1.5	83
50	Study of alkyl chain length dependent characteristics of imidazolium based ionic liquids [CnMIM]+[TFSA]â^' by Brillouin and dielectric loss spectroscopy. Current Applied Physics, 2013, 13, 271-279.	1.1	16
51	Bifunctional Gd2O3:Er3+ particles with enhanced visible upconversion luminescence. Journal of Alloys and Compounds, 2013, 572, 113-117.	2.8	34
52	Fabrication of bifunctional core-shell Fe3O4 particles coated with ultrathin phosphor layer. Nanoscale Research Letters, 2013, 8, 357.	3.1	24
53	Cell-based capacitance sensor for analysis of EGFR expression on cell membrane. , 2013, , .		1

#	Article	IF	CITATIONS
55	Synthesis and luminescence properties of Ho3+ doped Y2O3 submicron particles. Journal of Physics and Chemistry of Solids, 2012, 73, 176-181.	1.9	30
56	Synthesis and Photoluminescence Properties of Ho ³⁺ Doped LaAlO3 Nanoparticles. Journal of Nanoscience and Nanotechnology, 2012, 12, 5847-5851.	0.9	12
57	Advantages of using Ti-mesh type electrodes for flexible dye-sensitized solar cells. Nanotechnology, 2012, 23, 225602.	1.3	38
58	Tailoring the luminescent properties of Gd2O3:Tb3+ phosphor particles by codoping with Al3+ ions. Journal of Alloys and Compounds, 2012, 541, 263-268.	2.8	38
59	Synthesis and optical properties of Gd2O3:Pr3+ phosphor particles. Journal of Sol-Gel Science and Technology, 2012, 64, 156-161.	1.1	9
60	The optical properties of Eu3+ and Tm3+ codoped Y2O3 submicron particles. Journal of Alloys and Compounds, 2012, 525, 8-13.	2.8	24
61	Compressed-exponential relaxations in supercooled liquid trehalose. Current Applied Physics, 2012, 12, 1548-1552.	1.1	4
62	Color-tunable properties of Eu3+- and Dy3+-codoped Y2O3 phosphor particles. Nanoscale Research Letters, 2012, 7, 556.	3.1	61
63	Synthesis and optical properties of Dy3+-doped Y2O3 nanoparticles. Journal of the Korean Physical Society, 2012, 60, 244-248.	0.3	29
64	Facile synthesis of bifunctional silica-coated core–shell Y2O3:Eu3+,Co2+ composite particles for biomedical applications. RSC Advances, 2012, 2, 9495.	1.7	37
65	Cytotoxicity and cell imaging potentials of submicron colorâ€ŧunable yttria particles. Journal of Biomedical Materials Research - Part A, 2012, 100A, 2287-2294.	2.1	12
66	Investigation of ultraviolet carrier recombination of Volmer-Weber type ZnO nanocrystals and nanorods through Varshni's formula and Arrhenius plots. Journal of the Korean Physical Society, 2012, 60, 466-471.	0.3	3
67	Submicron Y2O3 particles codoped with Eu and Tb ions: Size controlled synthesis and tuning the luminescence emission. Journal of Colloid and Interface Science, 2012, 373, 14-19.	5.0	30
68	Effect of nanoscale confinement on dielectric relaxations in a 3wt.% water-galactose mixture. Journal of the Korean Physical Society, 2012, 60, 1092-1096.	0.3	1
69	A facile route to aligned TiO2 nanotube arrays on transparent conducting oxide substrates for dye-sensitized solar cells. Journal of Materials Chemistry, 2011, 21, 5062.	6.7	47
70	Optical and Electrical Properties of Ultralong ZnO Nanorod Fabricated from Preheating Hydrothermal Method. Journal of Nanoscience and Nanotechnology, 2011, 11, 463-469.	0.9	1
71	Unusual Melting Transition of Nitrogen Physisorbed on Carbon Nanotube Bundles. Journal of Nanoscience and Nanotechnology, 2011, 11, 6580-6583.	0.9	1
72	Enhanced Stokes and Anti-Stokes Photoluminescence Emission from LaAlO ₃ :Nd ⁺³ Nanosized Powder Coated with a SiO ₂ Shell Layer. Journal of Nanoscience and Nanotechnology, 2011, 11, 5892-5897.	0.9	4

#	Article	IF	CITATIONS
73	Effects of the Nano-Tubular Anodic TiO ₂ Buffer Layer on Bioactive Hydroxyapatite Coating. Journal of Nanoscience and Nanotechnology, 2011, 11, 286-290.	0.9	3
74	Improved conversion efficiency of dye-sensitized solar cell based on the porous anodic TiO2 nanotubes. Current Applied Physics, 2011, 11, S320-S323.	1.1	6
75	Effects of the disaccharide concentration and the extrusion speed on the size of unilamella vesicles. Current Applied Physics, 2011, 11, 1401-1404.	1.1	0
76	The structural and optical properties of Volmer–Weberâ€ŧype ZnO nanorods. Physica Status Solidi (A) Applications and Materials Science, 2011, 208, 1021-1026.	0.8	5
77	Annealing Effects of Sapphire Substrate on the Structure and Properties of ZnO Films Grown via Pulsed Laser Deposition. Journal of Nanoscience and Nanotechnology, 2011, 11, 584-588.	0.9	1
78	Single-Crystalline Twinned ZnO Nanoleaf Structure via a Facile Hydrothermal Process. Journal of Nanoscience and Nanotechnology, 2011, 11, 2175-2184.	0.9	3
79	Study of dielectric relaxations of anhydrous trehalose and maltose glasses. Journal of Chemical Physics, 2011, 134, 014508.	1.2	10
80	Effect of Annealing Ti Foil on The Structural Properties of Anodic TiO2 Nanotube Arrays. Journal of the Korean Physical Society, 2011, 58, 575-579.	0.3	4
81	Effect of Nano-scale Confinement on Dielectric Relaxation in a 3 wt.% Water-Galactose Mixture. New Physics: Sae Mulli, 2011, 61, 406-412.	0.0	1
82	A study of dielectric relaxations in galactose–water mixtures. Journal of Non-Crystalline Solids, 2010, 356, 2836-2841.	1.5	6
83	Solution-derived 40 µm vertically aligned ZnO nanowire arrays as photoelectrodes in dye-sensitized solar cells. Nanotechnology, 2010, 21, 195602.	1.3	134
84	Synthesis of Carbon Nanotube-CuxO(x=8, 64) Nanocrystal Composites. Journal of the Korean Physical Society, 2010, 56, 421-424.	0.3	2
85	The Cooperation Effect of Mixed PEGs with Different Molecular Weights on The Morphology of TiO2 Porous Thin Films. Journal of the Korean Physical Society, 2010, 56, 413-416.	0.3	0
86	Preparation and characterization of nanostructured composite films for organic light emitting diodes. Journal of Physics: Conference Series, 2009, 187, 012029.	0.3	6
87	Characterizations of Sodium Modified Potassium Lithium Niobate Crystal. Ferroelectrics, 2009, 382, 7-15.	0.3	1
88	A study on the Raman spectra of Al-doped and Ga-doped ZnO ceramics. Current Applied Physics, 2009, 9, 651-657.	1.1	73
89	The growth mechanism and optical properties of ultralong ZnO nanorod arrays with a high aspect ratio by a preheating hydrothermal method. Nanotechnology, 2009, 20, 155603.	1.3	161
90	The Fabrication of TiO2 Mesoporous Thick Films by Employing a Pre-Embedded ZnO Nanorods Support. Journal of Nanoscience and Nanotechnology, 2009, 9, 7145-9.	0.9	1

#	Article	IF	CITATIONS
91	Fabrication of Volmer-Weber Type ZnO Nanorods by Combining RF Sputtering and Hydrothermal Methods. Journal of Nanoscience and Nanotechnology, 2009, 9, 6993-7.	0.9	2
92	Temperature dependent vibrational modes of glycosidic bond in disaccharide sugars. Carbohydrate Research, 2008, 343, 660-667.	1.1	6
93	Morphology transformation from ZnO nanorod arrays to ZnO dense film induced by KCl in aqueous solution. Thin Solid Films, 2008, 517, 626-630.	0.8	11
94	Controlled growth of ZnO nanorod templates and TiO2 nanotube arrays by using porous TiO2 film as mask. Journal of Sol-Gel Science and Technology, 2008, 47, 187-193.	1.1	12
95	Preparation and electrochemical characterization of porous SWNT–PPy nanocomposite sheets for supercapacitor applications. Synthetic Metals, 2008, 158, 638-641.	2.1	53
96	A Study of the Secondary Relaxation in Galactose-Water Mixtures. AIP Conference Proceedings, 2008, ,	0.3	1
97	Effects of Disaccharide Sugars on Dynamics of Water Molecules: Dynamic Light Scattering and Dielectric Loss Spectroscopy Studies. AIP Conference Proceedings, 2008, , .	0.3	0
98	Facile Covalent Attachment of Well-Defined Poly(<i>t</i> -butyl acrylate) on Carbon Nanotubes via Radical Addition Reaction. Journal of Nanoscience and Nanotechnology, 2008, 8, 4598-4602.	0.9	9
99	Structural and Electronic Characteristics of ZnO Thin Films dc Sputtered on Sapphire (0001) Substrates. Journal of the Korean Physical Society, 2008, 52, 1685-1688.	0.3	1
100	Covalent attachment of polystyrene on multi-walled carbon nanotubes via nitroxide mediated polymerization. Composite Interfaces, 2007, 14, 493-504.	1.3	11
101	Oxidation study of polycrystalline InN film using in situ X-ray scattering and X-ray photoemission spectroscopy. Thin Solid Films, 2007, 515, 4691-4695.	0.8	12
102	A Study of Structures in ZnO and ZnO:V2O5 Thin Films by In-Situ Synchrotron X-ray Scattering. Journal of the Korean Physical Society, 2007, 51, 862.	0.3	3
103	Growth Dynamics and Size Distribution of Self-Assembled ZnO Nanocrystals on a Metal Pt(111) Substrate. Journal of the Korean Physical Society, 2007, 51, 887.	0.3	2
104	Quick Phase Search Method on an Adsorbed System. Journal of the Korean Physical Society, 2007, 50, 1281.	0.3	1
105	A Study of the Structure in a ZnO/MgO Multilayer by Using a Synchrotron X-ray Scattering Method. Journal of the Korean Physical Society, 2007, 51, 866.	0.3	0
106	Influence of the Interface Property on the Memory Function in a CER Cell Based on Pr0.7Ca0.3MnO3 Films. Journal of the Korean Physical Society, 2007, 51, 545-549.	0.3	0
107	The secondary relaxation in the dielectric loss of glucose–water mixtures. Journal of Non-Crystalline Solids, 2006, 352, 4679-4684.	1.5	11
108	The liquid–glass transition in sugars: Relaxation dynamics in trehalose. Journal of Non-Crystalline Solids, 2006, 352, 4464-4474.	1.5	24

#	Article	IF	CITATIONS
109	The glass transition temperatures of sugar mixtures. Carbohydrate Research, 2006, 341, 2516-2520.	1.1	45
110	Nano-Particle Size Measurement by Photon Correlation Spectroscopy and Dielectric Loss Spectroscopy. AIP Conference Proceedings, 2006, , .	0.3	1
111	The Liquid Glass Transition in Sugars and Sugar Mixtures. AIP Conference Proceedings, 2006, , .	0.3	4
112	Dehydration Processes of Sugar Glasses and Crystals. AIP Conference Proceedings, 2006, , .	0.3	0
113	Covalent attachment of poly(ethylene glycol) on multi-walled carbon nanotubes. Composite Interfaces, 2006, 13, 321-328.	1.3	6
114	Strain effects in ZnO thin films and nanoparticles. Journal of Applied Physics, 2006, 99, 064308.	1.1	46
115	Morphological and structural characterization of epitaxial α-Fe2O3 (0001) deposited on Al2O3 (0001) by dc sputter deposition. Journal of Vacuum Science and Technology A: Vacuum, Surfaces and Films, 2005, 23, 1450-1455.	0.9	12
116	Quantum confinement in Volmer–Weber-type self-assembled ZnO nanocrystals. Applied Physics Letters, 2005, 86, 193113.	1.5	35
117	Low Frequency Impedance Study of Li2B4O7Single Crystals. Ferroelectrics, 2005, 326, 109-112.	0.3	Ο
118	Jamming transition in a highly dense granular system under vertical vibration. Physical Review E, 2005, 72, 011302.	0.8	15
119	Effects of Oxygen Pressure on the Crystalline of ZnO Films Grown on Sapphire by PLD Method. Journal of the Korean Physical Society, 2005, 47, 300.	0.3	16
120	Solubility of V2O5 in Polycrystalline ZnO with Different Sintering Conditions. Journal of the Korean Physical Society, 2005, 47, 333.	0.3	4
121	Transient Behavior of DC and AC Conductance in Li2B4O7 Single Crystals. Journal of the Korean Physical Society, 2005, 47, 317.	0.3	2
122	Near-edge x-ray absorption fine structure and x-ray photoemission spectroscopy study of the InN epilayers on sapphire (0001) substrate. Journal of Applied Physics, 2004, 95, 5540-5544.	1.1	19
123	Study of dielectric relaxations in glucose-water mixtures. AIP Conference Proceedings, 2004, , .	0.3	Ο
124	Growth of Na modified potassium lithium niobate crystal by the Czochralski method. Journal of Crystal Growth, 2004, 270, 370-375.	0.7	5
125	Oxidation study of InN/sapphire (0001) film usingin-situ synchrotron X-ray scattering. Physica Status Solidi A, 2004, 201, 2777-2781.	1.7	7
126	Structural relation and epitaxial properties of hexagonal InN and oxidized cubic In2O3. Solid State Communications, 2004, 130, 397-400.	0.9	23

#	Article	IF	CITATIONS
127	Impurity band characteristics near the band edge of Al-doped ZnO. Journal of Applied Physics, 2004, 96, 1507-1510.	1.1	35
128	Study of the structural evolution in ZnO thin film by in situ synchrotron x-ray scattering. Journal of Applied Physics, 2004, 96, 1740-1742.	1.1	40
129	Making monosaccharide and disaccharide sugar glasses by using microwave oven. Journal of Non-Crystalline Solids, 2004, 333, 111-114.	1.5	23
130	Growth and properties of Li2B4O7 single crystals doped with Cu, Mn and Mg. Journal of Crystal Growth, 2003, 249, 483-486.	0.7	37
131	Growth of high-quality βll-Li3VO4 single crystals by the Czochralski method. Journal of Crystal Growth, 2003, 259, 115-120.	0.7	5
132	Study of Nitrogen Adsorbed on Open-Ended Nanotube Bundles. Journal of Physical Chemistry B, 2003, 107, 1540-1542.	1.2	42
133	Identification of hexagonal polycrystal in epitaxially grown InN by synchrotron x-ray diffraction and near-edge x-ray absorption fine structure spectroscopy. Applied Physics Letters, 2003, 82, 2981-2983.	1.5	5
134	Photoluminescence of polycrystalline ZnO under different annealing conditions. Journal of Applied Physics, 2003, 94, 5787-5790.	1.1	90
135	Dielectric properties of Li3VO4 single crystals grown by the Czochralski method. Journal of Applied Physics, 2003, 93, 1697-1700.	1.1	10
136	ac conductance of surface layer in lithium tetraborate single crystals. Journal of Applied Physics, 2003, 94, 7246-7249.	1.1	10
137	Rapid Estimation of the Height-Height Correlation Functions from the Synchrotron X-Ray and AFM Study of very Thin SnO2/α-Al2O3(0001) FILM. International Journal of Modern Physics B, 2003, 17, 1183-1187.	1.0	1
138	Raman Study of the Effects of Hydrogen Gas Annealing on PbTiO3Crystals. Japanese Journal of Applied Physics, 2003, 42, 1292-1296.	0.8	8
139	Synchrotron x-ray scattering study on the evolution of surface morphology of the InN/Al2O3(0001) system. Applied Physics Letters, 2002, 81, 475-477.	1.5	18
140	Electrical properties of Li2B4O7 single crystals in the [001] direction: Comparison between crystals grown from Li2CO3 and B2O3 mixed powder and from Li2B4O7 powder. Journal of Applied Physics, 2002, 92, 4644-4648.	1.1	16
141	Ferroelectric and Electric Properties of the PZT/ZnO Hybrid Thin Films. Ferroelectrics, 2002, 268, 11-16.	0.3	2
142	Synchrotron x-ray scattering study of lattice relaxation in InN epitaxial layers on sapphire(0001) during dc sputter growth. Journal of Applied Physics, 2002, 92, 5814-5818.	1.1	14
143	Study of the Strain in InN Thin Films Using Synchrotron X-Ray Scattering. Japanese Journal of Applied Physics, 2002, 41, 1932-1935.	0.8	5
144	Characterization of Buried Ultrathin Layer and Multilayer System by X-Ray Scattering. Japanese Journal of Applied Physics, 2002, 41, 3039-3042.	0.8	1

#	ARTICLE	IF	CITATIONS
145	Synchrotron x-ray scattering study of SnO ₂ thin film grown on sapphire. Journal of Materials Research, 2002, 17, 2417-2422.	1.2	3
146	Study of Argon Adsorbed on Open-Ended Carbon Nanotube Bundles. Journal of Physical Chemistry B, 2002, 106, 9000-9003.	1.2	25
147	Study of Nitrogen Adsorbed on Single-Walled Carbon Nanotube Bundles. Journal of Physical Chemistry B, 2002, 106, 3371-3374.	1.2	50
148	Dielectric Non-Linearity in the Tetragonal Direction of Li2B4O7 Single Crystals. Journal of the Physical Society of Japan, 2001, 70, 3119-3123.	0.7	3
149	Critical Thickness of AlN Thin Film Grown on Al2O3(0001). Japanese Journal of Applied Physics, 2001, 40, 4677-4679.	0.8	10
150	Critical thickness and surface oxidation of epitaxial AIN thin films. Integrated Ferroelectrics, 1999, 24, 129-137.	0.3	3
151	A two-inch dc/rf circular magnetron sputtering gun for a miniature chamber for an in situ experiment. Review of Scientific Instruments, 1998, 69, 1616-1621.	0.6	0
152	Study on the phases in Bi _(1 - x) Gd _x VO ₄ ceramics II. Ferroelectrics, 1990, 109, 185-190.	0.3	2
153	Study on the phases of RVO ₄ (R=Dy, Eu, Gd, Yb) ceramics. Ferroelectrics, 1990, 109, 191-195.	0.3	3
154	Study on the phase transitions in Bi _(1 - x) Gd _x VO ₄ ceramics I. Ferroelectrics, 1990, 109, 197-202.	0.3	3
155	Infrared reflection studies of γâ€ray irradiated NaNO2. Journal of Applied Physics, 1981, 52, 2808-2811.	1.1	0